Third International Conference on Sustainable Construction Materials and Technologies http://www.claisse.info/Proceedings.htm

Influence of crack width limitation on the chloride penetration resistance and global warming potential of concrete slabs

P. Van den Heede[1*], M. Maes[1] and N. De Belie[1]

[1] *Magnel Laboratory for Concrete Research, Ghent University, Belgium*
[*]*Technologiepark Zwijnaarde 904, B-9052 Ghent (Zwijnaarde), Belgium,*
philip.vandenheede@ugent.be, mathias.maes@ugent.be, nele.debelie@ugent.be

ABSTRACT

Service life predictions for concrete exposed to chloride-induced steel corrosion usually result from durability tests done on uncracked concrete. The almost natural presence of cracks is not taken into account. A chloride migration coefficient for uncracked concrete could only be used if the structure can be considered as uncracked. This research shows the effect of crack width limitation on chloride migration in concrete. The maximum crack width allowed should be less than 0.1 mm to have the seemingly uncracked condition. The extra amount of steel needed to achieve a crack width of 0.05 mm in a concrete slab results in a 35-43% increase of the global warming potential. The slab is preferably made of fly ash + silica fume concrete because of its low 28 day chloride migration coefficient (3.4×10^{-12} m²/s), its long expected service life (> 100 years) and its ability to partially heal 0.1 mm cracks.

Keywords. Concrete cracking, chloride penetration, service life, life cycle assessment

INTRODUCTION

Recent sustainability studies show that concrete's global warmig potential is mainly governed by its binder composition, strength and service life (Van den Heede and De Belie, 2012, Van den Heede et al., 2012). With respect to the latter, researchers are advised to implement data from durability tests into models that simulate the main deterioration mechanism of concrete's environment to estimate its life span. When looking at chloride induced corrosion, the end of service life is often equalled with steel depassivation. For this failure event the model of Fib Bulletin 34 (Fib, 2006) based on Fick's second law, looks straightforward. Experimental chloride migration coefficients can be used to estimate when the critical chloride concentration will reach the rebars and end service life. However, this approach does not take into account the unavoidable presence of cracks in concrete due to the mechanical loads applied. True, a structure should always be designed as such that the maximum allowed crack width (0.3 mm for a submerged marine environment according to Eurocode 2 (CEN, 2005)) is not exceeded. Nevertheless, even 0.3 mm wide cracks in the tensile zone of a concrete slab – the case study of this paper – can easily extend beyond the location of the rebars and therefore offer direct pathways for chlorides. As a consequence, it makes sense to limit the maximum crack width allowed even more. Of course, this design approach will have its implications on the amount of reinforcing steel needed and therefore on the environmental impact of the slab.

In this research, we conducted chloride migration tests on concrete representative mortar samples containing a crack of 0.3, 0.2 and 0.1 mm in width. This was done to see whether crack width reduction could decrease the chloride penetration around the crack significantly. If not, it may be necessary to aim for very fine crack widths that can heal autogenously. Literature shows a fast and complete natural crack closing for crack widths ≤ 0.05 mm in Ordinary Portland cement (OPC) mortars, OPC + 10% silica fume (SF) mortars and OPC + 30% fly ash (FA) mortars (Jaroenratanapirom and Sahamitmongkol, 2011). Since these three different binder types were also studied in our research, it is certainly relevant to consider the 0.05 mm crack width criterion in this research as well. In a next research phase, concrete slabs made with traditional concrete and fly ash + silica fume concrete were designed according to the most suitable crack width criterion. Then, a full probabilistic service life prediction cf. Fib Bulletin 34 (Fib, 2006) was performed in COMREL, followed by a life cycle assessment (LCA) in SimaPro. This calculation was done to see the effect of crack width limitation on the global warming potential of the studied concrete slabs.

EXPERIMENTAL PROGRAM

Concrete representative mortar mixes. Two concrete compositions were studied. Mix T(0.45) has a cement content and water-to-cement (W/C) ratio of 340 kg/m³ and 0.45, respectively. It is seen as the appropriate OPC reference concrete for exposure class XS2 (BIN, 2004). The exposure class corresponds with an environment where steel reinforced concrete is permanently submerged in sea water. As a consequence, the concrete is exposed to chlorides and this can induce steel corrosion. The other concrete mix is characterized by the same total binder content (340 kg/m³) as the OPC reference. Only now it consisted out of three different cementitious materials: 50% Portland cement, 40% FA and 10% SF. The water-to-binder ratio (W/B) equaled only 0.35. An equivalent mortar mix was designed for the two concrete compositions in accordance with the well-known MBE (Mortier de Béton Équivalent in French/Concrete Equivalent Mortar in English) method (Schwartzentruber et al., 2000). Within a MBE mortar mix, the gravel mass fractions of the corresponding concrete mix – in this case $f_{gravel\ 2/8}$ and $f_{gravel\ 8/16}$ – are replaced with the amount of sand $\Delta f_{sand\ 0/4}$ that has the same specific surface. This sand fraction can be calculated by means of Equation (1) in which $S_{gravel\ 2/8}$, $S_{gravel\ 8/16}$ and $S_{sand\ 0/4}$ represent the specific surface areas of the applied coarse aggregates and sand used in the studied concrete mixes.

$$\Delta f_{sand\ 0/4} = \frac{f_{gravel\ 2/8} \cdot S_{gravel\ 2/8} + f_{gravel\ 8/16} \cdot S_{gravel\ 8/16}}{S_{sand\ 0/4}} \tag{1}$$

Replacing the gravel 2/8 and gravel 8/16 by the much finer sand 0/4 obviously affects the water demand of the mortar. As a result, its required water amount needs to be adjusted in accordance with the difference in water absorption between the gravels and the sand. This can be done with Equation (2):

$$\Delta f_{water} = -f_{gravel2/8} \cdot A_{gravel2/8} - f_{gravel8/16} \cdot A_{gravel8/16} + \Delta f_{sand0/4} \cdot A_{sand0/4} \tag{2}$$

with $A_{gravel\ 2/8}$, $A_{gravel\ 8/16}$ and $A_{sand\ 0/4}$ the water absorption coefficients of the coarse aggregates and the sand. The measured water absorption coefficient and the specific surface areas are shown in Table 1. The resulting two MBE mortar compositions can be found there as well.

Table 1. Specific surface areas and water absorption coefficients of the sand and aggregates and MBE mortar mix proportions

	Sand 0/4	Gravel 2/8	Gravel 8/16
Specific surface area (m²/kg)	4.889	0.398	0.194
Absorption coefficient (-)	0.008	0.018	0.011
Composition	**MBE T(0.45)**	**MBE SF(0.35)**	
Sand 0/4 (kg/m³)	850.8	864.9	
CEM I 52.5 N (kg/m³)	340	170	
Fly ash (kg/m³)	-	136	
Silica Fume (kg/m³)	-	34	
Water (kg/m³)	136.5	102.2	
SP (ml/kg B)	3.0	14.0	
W/B (-)	0.40	0.30	
FA/B (%)	0	40	
SF/B (%)	0	10	
Strength class	C50/60	C55/67	

Manufacture of MBE mortar with an artificial crack. 15 cylindrical specimens (diameter: 110 mm, height: 53 mm) were made for each of the two MBE mortar mixes in PVC tube moulds: 3 samples without crack plus 3×4 samples containing an artificial crack as a result of putting thin metal plates with a nominal thickness of 0.1, 0.2 and 0.3 mm at a depth of 15 mm in the cylindrical moulds just before casting. Figure 1a shows a schematic of the mould setup with the metal plate fixed at the desired crack depth cf. (Mu, 2012). After casting, the specimens were kept at a constant temperature and relative humidity (RH) of 20 °C and 95 %, respectively. The metal plates were carefully removed from the samples after approximately 12 h whereupon the cylinders were demoulded. From then on, they were stored again under the same conditions until the age of 28 days.

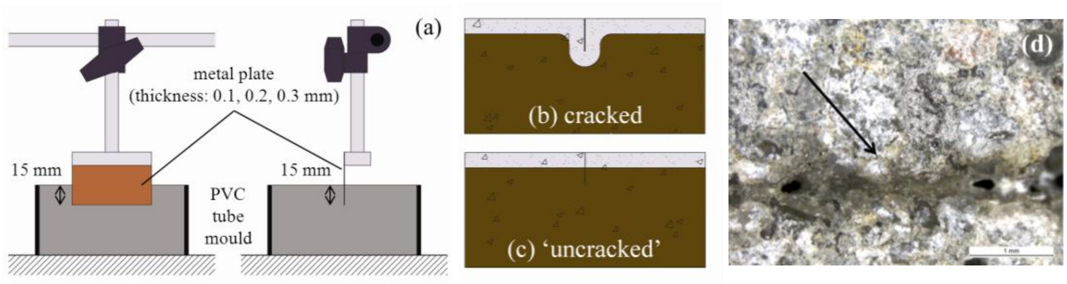

Figure 1. (a) Mould setup, (b) cracked sample, (c) seemingly uncracked sample, (d) partially healed 0.1 mm crack of MBE SF(0.35)

Microscopic crack width measurements. The obtained crack widths were measured after mechanical flattening of the cylinders' troweled surfaces and on the saw cut perpendicular to the crack of the fourth cylinder of each cracked series. The latter samples were only used for the evaluation of the cross-sectional crack width and not exposed to chlorides. All measurements were done with a Leica S8 APO stereo microscope (magnification: 2×) while using the LAS 3.7 software.

Chloride migration tests. A rapid chloride migration test was done in compliance with (NT Build 492, 1999). First, the cylindrical specimens were vacuum saturated in a 4 g/l

$Ca(OH)_2$ solution. After 18 ± 2 hours of immersion in this solution, the specimens were fixed inside silicon rubber sleeves with a 0.3 N NaOH (anolyte) solution on top. The bottom surface of the samples in the sleeves was brought in contact with a 10 % NaCl solution (catholyte). Then, an external electrical potential was applied axially across each cylinder, which forces the chloride ions to migrate into the specimens. After 24 hours the specimens were removed from the sleeves and split axially, whereupon a 0.1 M silver nitrate solution was sprayed onto the freshly split sections. When the white silver chloride precipitation had become clearly visible, the penetration depth was measured from the center to both edges at intervals of 10 mm. From the chloride ingress obtained, a non-steady state migration coefficient can be calculated with Equation (3):

$$D_{nssm} = \frac{0.0239(273+T)L}{(U-2)t}\left(x_d - 0.0238\sqrt{\frac{(273+T)Lx_d}{U-2}}\right) \tag{3}$$

where D_{nssm}, U, T, L, x_d and t represent the non-steady state migration coefficient (× 10^{-12} m²/s), the absolute value of the applied voltage (V), the average value of the initial and final temperatures in the anolyte solution (°C), the thickness of the specimen (mm), the average value of the penetration depths (mm) and the test duration (h), respectively.

D_{nssm} was only calculated for the uncracked MBE mortar samples. The cracked mortar specimens more or less went through the same test procedure except for the fact that the external electrical potential was imposed for only 4 h. This is much less than the normal 24 h test duration. The short test period was chosen to make sure that the overall chloride ingress would not be more than 13 mm, the average depth of the artificially induced cracks. Obviously, in case the crack width is too wide, the chloride penetration close to the crack would be higher than 13 mm (Figure 1b). The 10% NaCl solution would almost immediately reach the deepest point of the crack and chloride migration would start from there on. For each of the specimens containing a 0.1, 0.2 or 0.3 mm crack, it was evaluated whether the chloride penetration around the crack extended much beyond its deepest point. If not, the specimen could be considered as uncracked (Figure 1c) and the D_{nssm} value measured for the uncracked specimen would also be valid. As such, service life prediction could be done using D_{nssm} values measured on uncracked concrete. However, it also means that a concrete structure needs to be designed according to the stricter maximum crack width criterion.

CRACK WIDTH REDUCTION IN CONCRETE SLABS

When designing a concrete slab for a given mechanical load, an evaluation of the expected crack width in the service limit state is imperative. Eurocode 2 (CEN, 2005) provides an Equation (4) to calculate a characteristic crack width w_k (mm) for the structural element under investigation.

$$w_k = \left(3.4\cdot c + 0.425\cdot k_1\cdot k_2\cdot\frac{\Phi}{\frac{A_s}{A_{c,eff}}}\right)\cdot\left(\frac{\sigma_s}{E_s} - k_t\cdot\frac{f_{ct,eff}}{\frac{A_s}{A_{c,eff}}\cdot E_s}\cdot\left(1+\alpha\cdot\frac{A_s}{A_{c,eff}}\right)\right) \tag{4}$$

with c: concrete cover d + 10 mm, factor k_1: 0.8, factor k_2: 0.5, Φ: diameter of the rebar, A_s: cross-sectional area of the steel (mm²), $A_{c,eff}$: effective cross-sectional area of the concrete in the tensile zone (mm²), σ_s: steel stress (N/mm²), E_s: design value for steel's modulus of elasticity, factor k_t: 0.4, $f_{ct,eff}$: concrete's effective tensile strength (N/mm²), α: effective ratio of the moduli of elasticity for steel and concrete.

Eurocode 2 imposes a characteristic crack width of 0.3 mm for exposure class XS2 (CEN, 2005). For a given diameter of the rebars, the characteristic crack width can be reduced by increasing the overall steel cross-sectional area. Thus, more rebars would be needed to meet stricter crack width criteria.

SERVICE LIFE PREDICTION

Fib Bulletin 34 (Fib, 2006) is a design code providing the necessary models for a full probabilistic service life prediction. The design approach consists of defining a suitable limit state Equation (5) containing the necessary load and resistance variables for the deterioration mechanism under investigation, in this case chloride induced corrosion:

$$C_{cr} = C_0 + (C_{S,\Delta x} - C_0) \cdot \left[1 - \text{erf} \frac{d - \Delta x}{2 \cdot \sqrt{D_{app,C} \cdot t}} \right] \tag{5}$$

with C_{cr}: the critical chloride content (wt.-%/binder), C_0: the initial chloride content (wt.-%/binder), $C_{S,\Delta x}$: chloride content at depth Δx (wt.-%/binder), d: concrete cover, Δx: depth of the convection zone (mm), t: time (years), erf(.): error function and $D_{app,C}$: apparent coefficient of chloride diffusion through concrete (mm²/years). The latter coefficient can be obtained from the experimental non-steady state migration coefficient using Equation (6):

$$D_{app,C} = \exp\left(b_e \left(\frac{1}{T_{ref}} - \frac{1}{T_{real}} \right) \right) \cdot D_{RCM,0} \cdot k_t \cdot \left(\frac{t_0}{t} \right)^a \tag{6}$$

with b_e: a regression variable (K), T_{ref}: the standard test temperature (K), T_{real}: the temperature of the structural element or the ambient air (K), $D_{RCM,0}$: the non-steady state chloride migration coefficient (mm²/years), k_t: a transfer parameter (-), t_0: a reference point of time (years), t: time (years) and a: the ageing exponent (-). A combination of (5) and (6) enables an estimation of the time to steel depassivation. Table 2 gives a quantification of all the input parameters which are normally used in the model.

Note that the critical chloride content (1.9 wt.-%/binder, cf. Duracrete, 2000) differs from the 0.6 wt.-%/binder prescribed by Fib Bulletin 34 (Fib, 2006). This value should be valid for submerged OPC concrete with W/C ratios ranging between 0.5 and 0.4. A parameter study conducted by (Van den Heede et al., 2012) showed that 1.9 wt.-%/binder is probably a more realistic than 0.6 wt.-%/binder. Since it is still uncertain whether the critical chloride content increases or decreases in the presence of FA or other cementitious materials (Angst et al., 2009), the same C_{cr} value was adopted for both T(0.45) and SF(0.35). Nevertheless, further investigation on the actual C_{cr} value for each concrete type is still imperative. The applied ageing exponents a (-) are the values suggested by Fib Bulletin 34 (Fib, 2006) for OPC (0.3) and FA (0.6) concrete in general. These values are not mix specific. It is not sure whether the latter value is also valid for FA+SF concrete. In Duracrete a characteristic ageing exponent of 0.62 is given for concrete that contains SF (Duracrete, 2000). For now, we decided to use the lowest of these two values as the ageing exponent of FA+SF concrete. More accurate mix specific ageing exponents could be calculated from non-linear regression analyses based on chloride diffusion coefficients obtained at different ages. Their experimental determination is for the moment still ongoing.

Table 2. Quantification of the input parameters for the limit state equation defined by (5) and (6)

Parameter	distribution	mean	stdv	Lower bound	Upper bound
C_{cr} (wt.-%/binder)	Beta	1.9	0.15	0.2	2.0
C_0 (wt.-%/binder)	Constant	0	-	-	-
$C_{S,\Delta x}$ (wt.-%/binder)	Normal	3.0	0.8	-	-
d (mm)	Lognormal	40	8	-	-
Δx (mm)	Constant	0	-	-	-
b_e (K)	Normal	4800	700	-	-
T_{ref} (K)	Constant	293	-	-	-
T_{real} (K)	Normal	283	5	-	-
$D_{RCM,0}$ (mm²/yrs)	Normal	**336.2 (MBE T(0.45))** **107.5 (MBE SF(0.35))**	**32.2** **20.2**	- -	- -
k_t (-)	Constant	1	-	-	-
t_0 (yrs)	Constant	0.0767 (28d)	-	-	-
a (-)	Beta	0.30 (OPC) 0.60 (FA)	0.12 0.15	0.0 0.0	1.0 1.0

The probabilities of failure (P_f) and reliability indices (β) that result from the limit state equation defined by (5) and (6) were calculated using the First Order Reliability Method (FORM) available in the probabilistic COMREL software. In compliance with Fib Bulletin 34 (Fib, 2006), these parameters need to meet the requirements for the depassivation limit state ($P_f \leq 0.10$ and $\beta \geq 1.3$) to qualify for use in a XS2 environment.

LIFE CYCLE ASSESSMENT

In compliance with ISO 14040 (ISO, 2006), the LCA consisted of four major steps: definition of goal and scope, inventory analysis, impact analysis and interpretation.

Definition of goal and scope. This LCA was conducted to quantify the reduction in greenhouse gas emissions that result from replacing 50% of concrete's OPC with 40% FA and 10% SF fume while taking into account the differences in strength and durability with OPC concrete. Therefore, a concrete slab located in a submerged marine environment carrying a variable load of 5 kN/m² was chosen as functional unit. The strength classes of the two studied MBE mortars (Table 1) were assumed to be similar to the strength classes of their corresponding concrete compositions. The same strength classes were considered in the design of the concrete slab (span: 5 m, width: 1 m). Ribbed steel bars with a diameter of 16 mm and steel quality 500 were used as reinforcements. All design calculations were done in accordance with Eurocode 2 (CEN, 2005). Another reason for choosing a concrete slab as functional unit is because this type of structural element allows for a crack controlled design. As a result, it can be calculated how much extra reinforcing steel would be needed to obtain a slab where the concrete in the tensile zone would behave as uncracked cf. the drawing in Figure 1c. Only for a slab designed as such, a service life prediction based on the chloride migration tests performed on uncracked concrete samples would be valid. Thus, a quantification of the additional environmental impact attributed to the crack-controlling efforts done to enable the use of chloride migration coefficients for uncracked concrete as input to the service life prediction models would be very useful. With our functional unit choice this aspect can be included as well.

Inventory analysis. Per concrete constituent, the necessary inventory data were collected from the Ecoinvent database (Frischknecht and Jungbluth, 2007). Their proper short descriptions as mentioned in the database together with the amounts used to manufacture 1 m³ of each concrete mix, are shown in Table 3.

Table 3. Overview of the life cycle inventory data used per concrete mix

Material data (kg)	**Distribution**	**T(0.45)**	**SF(0.35)**
Sand, at mine/CH U	Normal	766 ± 44	778 ± 45
Gravel, round, at mine/CH U	Normal	1135 ± 109	1154 ± 111
Portland cement, strength class Z 52.5, at plant/CH U	Constant	340	170
Fly ash[a]	Constant	-	136
Silica fume[b]	Constant	-	34
Tap water, at user/CH U	Constant	153	119
Superplasticizer (EFCA 2006)	Constant	1.1	5.2
Processing data (kWh)	**Distribution**	**T(0.45)**	**SF(0.35)**
Electricity, low voltage, production BE, at grid/BE U	Constant	3.83	3.83

[a] patially contains Ecoinvent data: 'Electricity, hard coal, at power plant/BE U', through allocation
[b] partially contains Ecoinvent data: 'MG-silicon, at plant/NO U', through allocation

Mean values and standard deviations for the sand and aggregates were calculated from the amounts of each material needed according to Fuller's optimal particle size distribution curve for three deliveries of sand and aggregates to our laboratory. The probabilistic distribution of these amounts is assumed to be normal. The amounts of cement, FA, water and superplasticizer (SP) were assumed to be accurately weighed and therefore considered as constants. For the allocation of impacts attributed to FA, the economic allocation coefficient (= 1.0 % of the impact of coal fired electricity production associated with 1 kg FA) as proposed by (Chen et al., 2010) was applied. For 1 kg SF, the economic allocation coefficient should equal 4.8% of the impact of Si metal production (Chen, 2009). SP inventory data were obtained from an environmental declaration published by the European Federation of Concrete Admixture Associations (EFCA, 2006). The transport of each constituent to the concrete plant was not incorporated in the LCA since its environmental impact is always very case specific. With respect to the steel reinforcements the following Ecoinvent inventory data were used: 'Reinforcing steel, at plant/RER U'.

Impact analysis and interpretation. The IPCC 2007 GWP 100a impact method was used to calculate the Global Warming Potential (GWP) expressed in kg CO_2 equivalents for a timeframe of 100 years. All calculations were done in the LCA software SimaPro 7.3.3.

RESULTS AND DISCUSSION

Microscopically measured crack widths. Table 4 shows that the observed crack widths at the surface did not differ much from the thicknesses of the thin metal plates (0.1, 0.2 and 0.3 mm). The cross-sectional crack widths measured on one cylinder of each cracked series further confirm this good match for both mortar compositions. Note that the cross-sectional crack width observed on the MBE SF(0.35) sample with a 0.1 mm crack had a rather high standard deviation on the individual values (stdv.: 0.08 mm). This is mainly due to the fact that there were 'zero' measurements. At several places alongside its cross-sectional area, the crack showed obvious signs of closure which could not be attributed to a mere filling of the crack by loose particles originating from the mechanical surface flattening (Figure 1d). This finding indicates that for a crack width of ± 0.1 mm, partial autogenous crack healing can occur. Since this phenomenon was not observed on the MBE T(0.45) sample with a 0.1 mm crack, the partial autogenous healing that was detected is most likely induced by further hydration of the unreacted alternative binders present in MBE SF(0.35). Fast natural healing of cracks ≥ 0.05 mm in OPC mortars with 10 % silica fume was reported by (Jaroenratanapirom and Sahamitmongkol, 2011). Figure 1d indicates that this may also be the case for the MBE SF(0.35) mortar containing 50% OPC, 40% FA and 10% SF. However, further research is needed to find further confirmation for this statement.

Table 4. Microscopic crack width measurements

MBE T(0.45)			**MBE SF(0.35)**		
0.1 mm	**Flattened surface**	**Cross-section**	**0.1 mm**	**Flattened surface**	**Cross-section**
n	33	12	n	33	12
mean	0.08 mm	0.09 mm	mean	0.13 mm	0.12 mm
stdv.	0.01 mm	0.01 mm	stdv.	0.03 mm	0.08 mm
0.2 mm	**Flattened surface**	**Cross-section**	**0.2 mm**	**Flattened surface**	**Cross-section**
n	33	12	n	33	12
mean	0.19 mm	0.21 mm	mean	0.21 mm	0.20 mm
stdv.	0.01 mm	0.02 mm	stdv.	0.02 mm	0.03 mm
0.3 mm	**Flattened surface**	**Cross-section**	**0.3 mm**	**Flattened surface**	**Cross-section**
n	33	12	n	33	12
mean	0.27 mm	0.34 mm	mean	0.29 mm	0.33 mm
stdv.	0.02 mm	0.02 mm	stdv.	0.03 mm	0.05 mm

Measured chloride migration coefficients. MBE mortar SF(0.35) is characterized by a 28 day non-steady state chloride migration coefficient D_{nssm} of $3.4 \pm 0.6 \times 10^{-12}$ m²/s. This is only around one third of the 28 day D_{nssm} value ($10.7 \pm 1.0 \times 10^{-12}$ m²/s) obtained for OPC reference MBE T(0.45). Thus, when uncracked, the former mortar composition is much more resistant to chloride penetration than the latter. In terms of service life, this finding suggests that less rehabilitation actions (repair/replacement) will be needed for an uncracked fly ash+silica fume concrete slab exposed to seawater within a 100 years timeframe. To evaluate this quantitatively, the D_{nssm} values were expressed in mm²/years and used as $D_{RCM,0}$ input (Table 2) to the service life prediction model defined by Equations (5) and (6).

Determination of the maximum crack width allowed. Figure 2 shows one representative photo of the chloride penetration for each mortar-crack combination. Per mortar mix and crack width all broken cylinder surfaces (n = 6) looked similar. The chloride penetration always extended beyond the deepest point of the crack. This was the case for all three nominal crack widths (0.1, 0.2, 0.3 mm) that were experimentally assessed in this research, also when already some partial autogenous healing had occurred for the 0.1 mm crack of MBE SF(0.35). In other words, none of the studied cracked samples could be considered as uncracked cf. Figure 1c. This means that within the slab design, the maximum crack width allowed should be reduced even more, preferably to a value that ensures complete autogenous healing of the crack, i.e. the 0.05 mm crack width suggested by (Jaroenratanapirom and Sahamitmongkol, 2011). Obviously, it would have been better to manufacture another series of cracked samples containing a 0.05 mm crack and subject them to chloride migration tests as well. However, it is difficult to implement such cracks in mortar using very thin metal plates with a thickness of only 0.05 mm. More research is needed first on how this could be achieved in the future.

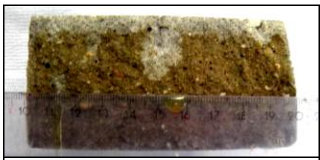		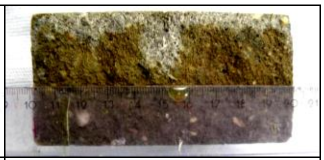
MBE T(0.45)_0.1 mm	MBE T(0.45)_0.2 mm	MBE T(0.45)_0.3 mm
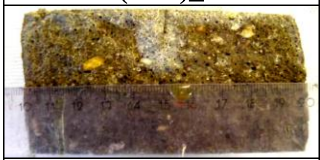		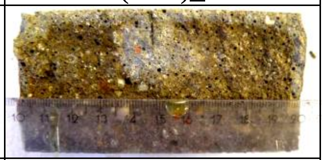
MBE SF(0.35)_0.1 mm	MBE SF(0.35)_0.2 mm	MBE SF(0.35)_0.3 mm

Figure 2. Chloride penetration for the cracked samples

Concrete slab dimensioning. When following Eurocode 2 (CEN, 2005), the slab made with T(0.45) concrete should have a thickness of 150 mm and contain 6 rebars with a 16 mm diameter. For the slab made with SF(0.35), the slab thickness can be reduced to 140 mm due to the higher strength class of the concrete. The required number of rebars remained the same. Under these conditions, the estimated crack widths in the tensile zone equaled 0.18 and 0.21 mm, respectively. To reduce the theoretical crack width of the two slabs to 0.05 mm – the value proposed by (Jaroenratanapirom and Sahamitmongkol, 2011) – the necessary number of rebars would need to be increased to 14 and 15, respectively.

Service life prediction. Comparing the reliability indices β and probabilities of failure P_f with the prescribed criteria ($\beta \geq 1.3$ and $P_f \leq 0.1$) leads to the following findings. It shows that the estimated service life of MBE T(0.45) is much lower than 100 years (25 years). While for MBE SF(0.35) the predefined service life of 100 years ($\beta = 2.7$ and $P_f = 0.003$) is exceeded by far. This means that a concrete slab made out of T(0.45) concrete will need a certain number of rehabilitation actions within the 100 years time span. For this case study it was assumed that rehabilitation comprised complete replacement of the slab, and not local repair. The concrete and steel needed for three T(0.45) slab replacements need to be included in the LCA study to have a correct, durability related environmental impact calculation. Since a 100 years service life seems easily achievable for composition SF(0.35), only the concrete volume for the initial manufacture of the slab needs to be considered in the LCA.

Life cycle assessment. Without active crack width limitation, the GWPs of the T(0.45) and SF(0.35) concrete slabs (inclusive the required slab replacements within a 100 years life span) amounts to 1120 ± 116 and 227 ± 14 kg $CO_{2\,eq}$, respectively. Increasing the amount of reinforcing steel to 14 and 15 rebars to achieve a characteristic crack width of only 0.05 mm, will increase the environmental score substantially with 35% and 43%, respectively.

CONCLUSIONS

In uncracked condition, a concrete representative FA+SF mortar is characterized by a very low chloride migration coefficient after 28 days (3.4×10^{-12} m²/s) which highly contributes to the estimated long service life (> 100 years). As a result, a slab made with the corresponding FA+SF concrete has a much lower GWP (– 80%) when compared with a OPC reference concrete slab. To correct for the unavoidable presence of cracks in such a slab, the additional amount of reinforcing steel needed to reduce the characteristic crack width to 0.05 mm, a value that should ensure fast and complete autogenous crack healing, needs to be included in the LCA as well. This extra impact should be considered when service life prediction is based on chloride migration coefficients measured on uncracked concrete/ mortar. The extra steel can increase the GWP of the FA+SF concrete slab with another 43%.

ACKNOWLEDGEMENTS

The authors would like to thank Ghent University for the research funding. The PhD grant of Mathias Maes is funded by the Agency for Innovation by Science and Technology (IWT).

REFERENCES

Angst, U., Elsener, B., Larsen, C. K. and Vennesland, O. (2009). "Critical Chloride Content in Reinforced Concrete – A review." *Cem Concr Res*, 39(12): 1122-1138.

BIN. (2004). *NBN B15-001, Supplement to NBN EN 206-1, Concrete – specification, performance, production and conformity*, BIN, Brussels.

CEN. (2005). *NBN EN 1992-1-1, Eurocode 2,: Design of concrete structures – Part 1-1: General rules and rules for buildings (+AC: 2008)(+AC: 2010)*, CEN, Brussels.

Chen, C. (2009). *A study of traditional and alternative structural concretes by means of the life cycle assessment method (in French)*, PhD thesis, UTT, Troyes.

Chen, C., Habert, G., Bouzidi, Y., Jullien, A., and Ventura, A. (2010). "LCA allocation procedure used as an incitative method for waste recycling : An application to mineral additions in concrete." *Resour Conserv Recy*, 54 (12): 1231-1240.

Duracrete. (2000). *Probabilistic performance based durability design of concrete structures: General guidelines for durability design and redesign*, CUR, Gouda.

EFCA. (2006). "EFCA Environmental Declaration Superplasticizing Admixtures (2006)." *EFCA*, http://www.efca.info/publications.html>(Aug. 26, 2011).

Fib. (2006). *Fib Bulletin 34, Model code for service life design*, Fib, Lausanne.

Frischknecht, R., and Jungbluth, N., Eds. (2007) *Overview and methodology, Final report ecoinvent v2.0 No. 1*, Swiss Centre for Life Cycle Inventories, St-Gallen.

ISO. (2006). ISO 14040, *Environmental management – Life cycle assessment – principles and framework*, ISO, Geneva.

Jaroenratanapirom, D., and Sahamitmongkol, R. (2011). "Self-crack closing ability of mortar with different additives." *J Met Mater Miner*, 21(1): 9-17.

Mu, S. (2012) *Chloride penetration and service life prediction of cracked self-compacting concrete*, PhD thesis, Ghent University, Ghent

Nordtest (1999) *NT Build 492, Concrete, mortar and cement-based repair materials: chloride migration coefficient from non-steady state migration experiments*, Nordtest, Espoo.

Schwartzentruber, A., and Catherine, C. (2000). "Method of the concrete equivalent mortar (CEM) – A new tool to design concrete containing admixture (in French)." *Mater Struct*, 33(232): 475-482

Van den Heede, P., and De Belie, N. (2012). "Environmental impact and life cycle assessment (LCA) of traditional and 'green' concretes: Literature review and theoretical calculations." *Cem Concr Compos*, 34(4): 431-442.

Van den Heede, P., Maes, M., Gruyaert, E., and De Belie, N. (2012). "Full probabilistic service life prediction and life cycle assessment of concrete with fly ash and blast-furnace slag in a submerged marine environment: a parameter study." *Int J Environ Sust Dev*, 11(1): 32-49.